Dynamics of Diurnal Thermocline Formation in the Oceanic Mixed Layer

YIGN NOH

Department of Astronomy and Atmospheric Sciences, Yonsei University, Seoul, Korea

(Manuscript received 9 September 1993, in final form 3 February 1996)

ABSTRACT

Diurnal thermocline formation in the oceanic mixed layer under a stabilizing buoyancy flux is studied by numerical simulation of a turbulence model in which the interaction between turbulence structure and density stratification is taken into consideration, and the mechanism for its formation is clarified based on the results. From the simulations, the flux of turbulent kinetic energy is a dominant source of turbulence in the upper mixed layer and plays an indispensable role for the formation of a diurnal thermocline; below the diurnal thermocline, turbulence is maintained by shear production, which causes the growth of diurnal thermocline thickness. The flux Richardson number at the diurnal thermocline maintains a constant value (about unity), regardless of the shear stress and buoyancy flux at the sea surface, and the diurnal thermocline depth grows more slowly than predicted by the Monin–Obukhov length scale. The model results are compared with the observational data, and the assumptions introduced in various mixed layer models are reexamined in view of these results.

1. Introduction

When a stabilizing heat flux and the generation of turbulence exist simultaneously at the sea surface, work is required against the buoyancy force; this reduces the turbulent kinetic energy (TKE) in the oceanic mixed layer. The buoyancy force becomes more important with increasing depth, and at a certain depth balances the influx of TKE, where a diurnal (or seasonal) thermocline forms (see, for example, Turner 1981). Once a diurnal thermocline is formed due to surface heat flux, all the vertical transports from the sea surface, such as heat, turbulent kinetic energy, and dissolved oxygen, are suppressed at the thermocline and limited to a thin mixed layer above. The formation of a diurnal thermocline, therefore, plays important roles for upper ocean dynamics, and accurate information is essential to predict the sea surface temperature and the vertical transport of heat, momentum, dissolved gases, biological mass, etc.

It has been suggested that the depth at which a diurnal thermocline is formed is proportional to the Monin–Obukhov length scale (Kitaigorodskii 1970); that is,

$$L = u_*^3/Q. \qquad (1.1)$$

Here u_* is the frictional velocity determined by wind stress τ, or $u_* = (\tau/\rho_0)^{1/2}$, where ρ_0 is the mean density of sea water. The buoyancy flux at the sea surface, Q, arises from sensible and latent heat fluxes, radiation, evaporation, and precipitation (Phillips 1977).

Detailed accounts of the formation of a diurnal thermocline are recorded in several field studies (Delnore 1972; Stommel et al. 1969; Imberger 1985; Schudlich and Price 1992; Brainerd and Gregg 1993a). In particular, recent measurements of the oceanic microstructure by Brainerd and Gregg (1993a) revealed several novel features, giving insight into the upper ocean process during the formation of a diurnal thermocline. They found that the mean density field within the mixed layer above the diurnal thermocline remains stratified with $N^2 \lesssim 1.5 \times 10^{-5}$ s^{-2}, which increases to $N^2 \approx 5.4 \times 10^{-5}$ s^{-2} at the diurnal thermocline. They also found that the thickness of a diurnal thermocline increases with time, from about 2 m at its formation to nearly 7 m, whereas the mixed layer above the diurnal thermocline maintains a constant thickness of 7–8 m. Based on measurements of vertical profiles of dissipation rate, the turbulent kinetic energy above the diurnal thermocline greatly exceeds that estimated from the turbulence generation by velocity shear only, and, once the diurnal thermocline is formed, the TKE in the remnant layer below decreases slowly due to dissipation.

There have been numerous studies that attempted to simulate the variation of the oceanic mixed layer responding to atmospheric conditions (for a review, see Kraus 1988). In general, two different modeling approaches have been employed: 1) bulk models, in which the integrated properties over the entire mixed layer are considered assuming temperature and velocity profiles a priori (Kraus and Turner 1967; Denman and Miyake 1973; Kim 1976; Niiler and Kraus 1977; Gar-

Corresponding author address: Dr. Yign Noh, Dept. of Astronomy and Atmospheric Sciences, Yonsei University, 134 Shinchon-dong, Seodaemun-gu, 120-749 Seoul, Korea.

wood 1977; Woods and Barkmann 1986; Price et al. 1986; Gaspar 1988) and 2) turbulence models, in which turbulence terms such as Reynolds stress and eddy diffusivity are parameterized (Mellor and Durbin 1975; Kundu 1980; Klein and Coantic 1981; Andre and Lacarrere 1985). The main purpose of these studies has been to examine the deepening of the mixed layer resulting from increased wind stress or surface cooling. Meanwhile, shoaling of the mixed layer, or the formation of a diurnal thermocline under a stabilizing buoyancy flux, has not been investigated as much, although a few bulk models have been attempted for this situation (Garwood 1987; Kraus et al. 1988).

To overcome the problem of simulating diurnal thermocline formation, a rather artificial assumption was introduced into the bulk models that the rate of the deepening of the mixed layer is zero whenever the calculated value of it becomes negative. This assumption converts the prognostic equation predicting the evolution of the mixed layer depth to a diagnostic equation determining the equilibrium depth, which is regarded as the depth of a diurnal thermocline. This approach suffers from a too rapid shoaling of the mixed layer as well as the inability to account for the remnant layer left below. A more serious defect of this approach is that it is not possible to explain the formation of a diurnal thermocline from an initially uniform layer. The bulk models are, in fact, ill suited to describe the formation of a diurnal thermocline, which involves the generation of a new internal structure, because they deal with the adjustment of a given mixed layer under atmospheric conditions while presupposing a uniform density profile within the mixed layer. Turbulence models capable of producing the change of density profiles within the mixed layer have not yet been considered seriously in this situation.

Another fundamental question regarding the diurnal thermocline formation is its lack of similarity between the atmospheric boundary layer and the oceanic mixed layer in response to a stabilizing buoyancy flux. When a stabilizing buoyancy flux is imposed on the surface of the atmospheric boundary layer during the night, appears a continuous temperature profile with the large temperature gradient near the surface rather than a thermocline is formed (Andre et al. 1978; Yamada and Mellor 1975; Stull 1988). In contrast, a stabilizing buoyancy flux imposed on the sea surface during the day leads to the formation of a diurnal thermocline while maintaining a relatively uniform temperature profile above it. This suggests that a fundamentally different dynamical process exists between these two planetary boundary layers, although most turbulence models of the oceanic mixed layer have been developed in a way similar to those of the atmospheric boundary layer (Mellor and Durbin 1975; Kundu 1980; Klein and Coantic 1981; Andre and Lacarrere 1985).

On the other hand, it has not yet been resolved clearly what is primarily responsible for the mixed layer dynamics: the local production of TKE by velocity shear or the TKE flux from the sea surface (Garwood 1979). The TKE flux plays a dominant role in most bulk models (e.g., Kraus and Turner 1967; Niiler and Kraus 1977), whereas it is usually regarded as negligible in turbulence models (e.g., Mellor and Durbin 1975; Klein and Coantic 1981). However, the TKE flux plays an important role in the turbulence model for thermocline formation in shear-free turbulence (Noh and Fernando 1991; Noh 1993). Yet, the role of TKE flux remains to be investigated in oceanic mixed layers with mean velocity shear.

Therefore, a turbulence model is used to investigate thermocline formation in the oceanic mixed layer in the presence of shear stress and stabilizing buoyancy flux at the sea surface with the aim to understand the mechanism of its formation, particularly to answer the questions mentioned above. In section 2, the turbulence model is developed to simulate the formation of a diurnal thermocline. The results are described in section 3 for both cases with and without TKE flux. The depth of the diurnal thermocline and the flux Richardson numbers at that depth are also obtained. The results are compared with observational data, and a mechanism for the formation of a diurnal thermocline is suggested. In section 4, the effects of Coriolis force and the penetration of solar radiation are discussed. Finally, conclusions are given in section 5, while the assumptions introduced in several widely used mixed layer models are reexamined in view of the present results.

2. The model

The equations for the mean velocity U, the mean buoyancy B and the mean turbulent kinetic energy E can be written as (see, for example, Phillips 1977)

$$\frac{\partial U}{\partial t} = -\frac{\partial}{\partial z}\overline{uw} \tag{2.1}$$

$$\frac{\partial B}{\partial t} = -\frac{\partial}{\partial z}\overline{bw} \tag{2.2}$$

$$\frac{\partial E}{\partial t} = -\frac{\partial}{\partial z}\left[\overline{w\left(\frac{p}{\rho_0} + \frac{u_i u_i}{2}\right)}\right] - \overline{uw}\frac{\partial U}{\partial z} - \overline{bw} - \epsilon, \tag{2.3}$$

where horizontal homogeneity is assumed and the direction of the current is given by x. Here u_i ($i = 1, 2, 3$) is the fluctuating velocity ($u_3 = w$), b is the fluctuating buoyancy ($= -g\rho/\rho_0$), ρ and p are the fluctuations of density and pressure, ϵ is the dissipation rate of TKE, and z is directed downward from the sea surface. The first three terms on the rhs of (2.3) represent the flux of TKE (F), the production by mean velocity shear (P_s), and the decay or production by buoyancy flux (P_b), respectively. Since the main objective is to clarify the mechanism, many effects are excluded as

they are considered unimportant to the dynamical process of diurnal thermocline formation, for example, the Coriolis force, the penetration of solar radiation into the deeper region, etc. Further discussions of the effects of Coriolis force and the penetration of solar radiation will be given in section 4.

Introducing eddy viscosity and eddy diffusivity, (2.1)–(2.3) can be rewritten as

$$\frac{\partial U}{\partial t} = \frac{\partial}{\partial z}\left(K\frac{\partial U}{\partial z}\right), \tag{2.4}$$

$$\frac{\partial B}{\partial t} = \frac{\partial}{\partial z}\left(K_B\frac{\partial B}{\partial z}\right), \tag{2.5}$$

$$\frac{\partial E}{\partial t} = \frac{\partial}{\partial z}\left(K_E\frac{\partial E}{\partial z}\right) + K\left(\frac{\partial U}{\partial z}\right)^2 + K_B\frac{\partial B}{\partial z} - \epsilon. \tag{2.6}$$

Here K is the eddy viscosity for the Reynolds stress, and K_B and K_E are the eddy diffusivities for B and E. They can be modeled as

$$K = Sql \tag{2.7}$$

$$K_B = S_B ql \tag{2.8}$$

$$K_E = S_E ql, \tag{2.9}$$

where q is the rms velocity of turbulence, $=(2E)^{1/2}$, and l is the length scale of turbulence. The dissipation rate can be modeled as

$$\epsilon = Cq^3 l^{-1}. \tag{2.10}$$

As long as there is no stratification, the constants are taken as $S = 0.39$ $(=S_0)$, Pr $(=S/S_B) = 0.8$, σ $(=S/S_E) = 1.95$, and $C = 0.06$ $(=C_0)$, which are the same as in the level-2 model of Mellor and Yamada (1982); here subscripts 0 represent the values of the empirical coefficients at no stratification. Similar values have also been used in other models; for example, $S_0 = 0.33$, Pr $= 0.8$, $\sigma = 1.37$ and $C_0 = 0.04$ by Davies and Jones (1988).

However, the proportionality constants S, S_B, S_E, and C are affected by the density stratification of the fluid. In stably stratified fluids, the growth of the vertical length scale of turbulence is limited by the buoyancy length scale l_b $(=q/N$, where N is the Brunt–Väisälä frequency; i.e., $N^2 = -\partial B/\partial z)$, and the eddies larger than l_b are radiated as internal waves (Csanady 1964; Britter et al. 1983). The eddy viscosity is then estimated by

$$K \sim ql_b \sim ql\,\mathrm{Rt}^{-1/2}, \tag{2.11}$$

where $\mathrm{Rt} = (Nl/q)^2$ is the Richardson number for turbulent eddies. Using (2.11) at large Rt, S can be represented by

$$S/S_0 = (1 + c_1\,\mathrm{Rt})^{-1/2}, \tag{2.12}$$

with an empirical coefficient c_1. From the comparison of the model results with experimental data in the case of thermocline formation in shear-free turbulence (Noh and Fernando 1991), $C_1 = 0.3$. Similarly, the effect of stratification on C is given by

$$C/C_0 = (1 + c_1\,\mathrm{Rt})^{1/2}. \tag{2.13}$$

It is assumed that Pr and σ are independent of Rt, as it is known that the effects of stratification on them are very weak (Mellor and Yamada 1982).

The basic presumption made in (2.12) and (2.13) is that what determines the eddy diffusivity is the kinetic energy of eddies overcoming the stratification regardless of whether the turbulence is produced by velocity shear, buoyancy, or TKE fluxes. In contrast to this, the flux Richardson number Rf $(= -(S_B/S)(\partial B/\partial z)/(\partial U/\partial z)^2 = P_b/P_s)$, which is determined by the mean velocity and buoyancy profiles, was used in the Mellor and Yamada model (1982) to parameterize the effects of stratification on S, and in their level-2 model, it is given by

$$S = a_1\frac{1 - a_2\,\mathrm{Rf}}{1 - a_3\,\mathrm{Rf}}, \tag{2.14}$$

where a_1, a_2, and a_3 are constants. This parameterization is fundamentally different from (2.12) in that S becomes zero if the stratification increases to a certain level $(\mathrm{Rf} = a_2^{-1} = 0.19)$, whereas S given by (2.12) gradually decreases to zero with stratification but maintains a positive value. Eddies smaller than l_b are not strongly affected by stratification and contribute to turbulent mixing, but eddies larger than l_b are radiated as internal waves (Hopfinger 1987; Stillinger et al. 1983). Therefore, the eddy diffusivity may not go to zero, even if the flux Richardson number based on the integral length scale exceeds a critical value. A modified form of the Mellor and Yamada model suggested by Galperin et al. (1988) introduced a parameterization in terms of Rt. More discussion on the Mellor and Yamada model will be given in section 5.

For the case of the atmospheric boundary layer the length scale l was suggested by Blackadar (1962) as

$$l = \frac{\kappa(z + z_0)}{1 + \kappa(z + z_0)/l_0} \tag{2.15}$$

with

$$l_0 = \gamma\frac{\int_0^\infty zE^{1/2}dz}{\int_0^\infty E^{1/2}dz}, \tag{2.16}$$

where $\kappa = 0.4$, $\gamma = 0.1$, and z_0 is the roughness length scale, which is a few centimeters in general. This length scale has been often employed for the oceanic mixed layer too (Klein and Coantic 1981; Andre and Lacarrere 1985).

Since the sea surface is a moving boundary, at which turbulence is generated continuously through wave breaking, the roughness length scale z_0 is expected to be much larger than that of the atmospheric boundary layer. In particular, with values of z_0 as small as a few centimeters as in the atmospheric boundary layer, K and K_B become very small near the surface. This relationship is contrary to the observations that K is a maximum near the sea surface (Yu and O'Brien 1991) and that the temperature always remains relatively uniform for a few meters below the sea surface even under a stabilizing heat flux (Denman and Miyake 1973). Therefore, a rather large value of the turbulence length scale near the surface, $l(z = 0) = 1.4$ m, is assigned in the present model, based on the length scale near the sea surface calculated by Kundu (1980). The appropriateness of the length scale chosen will be corroborated in the later sections by comparison of the model results with the observational data.

The boundary conditions at the sea surface ($z = 0$) are given by

$$K\frac{\partial U}{\partial z} = u_*^2 \tag{2.17}$$

$$K_B\frac{\partial B}{\partial z} = Q \tag{2.18}$$

$$K_E\frac{\partial E}{\partial z} = mu_*^3. \tag{2.19}$$

The coefficient m, which determines the net TKE flux from the sea surface, has yet to be determined properly, although various values are suggested within the range $1 < m < 10$ (Kraus 1988; Klein and Coantic 1981). Since one of the main objectives of this paper is to investigate the importance of TKE flux, calculations are carried out with different cases of $m = 0$ and 10. Zero net fluxes of TKE, buoyancy, and momentum are assumed at the bottom.

In the steady state without both TKE flux and buoyancy flux, the production by mean velocity shear (P_s) and the dissipation rate (ϵ) are balanced locally. That is,

$$K\left(\frac{\partial U}{\partial z}\right)^2 - \epsilon = 0. \tag{2.20}$$

Integration of the momentum equation (2.4) in the steady state gives the momentum flux independent of depth such that

$$K\frac{\partial U}{\partial z} = u_*^2. \tag{2.21}$$

By eliminating $\partial U/\partial z$ from (2.20) and (2.21),

$$u_*^4/K = \epsilon, \tag{2.22}$$

which leads to the relation

$$q^2 = u_*^2/(SC)^{1/2} \tag{2.23}$$

from (2.7) and (2.10). The velocity profile in the neutrally stratified boundary layer is given by (Phillips 1977)

$$\frac{\partial U}{\partial z} = \frac{u_*}{\kappa(z + z_0)}, \tag{2.24}$$

when there is no TKE flux at the sea surface. By substituting (2.24) for $\partial U/\partial z$, (2.21) becomes

$$q = u_*/S, \tag{2.25}$$

using (2.15) with $l_0 = \infty$. The comparison of (2.23) with (2.25) gives

$$C = S^3, \tag{2.26}$$

which is consistent with the empirical values given in the present model.

First, the vertical profiles of U and E given by (2.24) and (2.25), which correspond to the case of no TKE flux, are applied to (2.4) and (2.6) in a homogeneous fluid ($B = 0$) under the imposed shear stress (2.17) and TKE flux (2.19). After an equilibrium state is obtained, the modified profiles of E and U are then used as the initial conditions for the model, together with $B = 0$.

3. Results

a. *Evolution of a thermocline with TKE flux ($m = 10$)*[1]

The time evolution of a buoyancy profile $B(z, t)$ is shown in Fig. 1a when typical values of the buoyancy flux $Q = 10^{-6}$ m^2 s^{-3} and the frictional velocity $u_* = 0.01$ m s^{-1} are used. Each graph corresponds to times $t = n\Delta t$ ($n = 1, 2, \cdots, 10$, $\Delta t = 10^3$ s). At early times ($n = 1$), an exponentially decreasing buoyancy distribution appears as in the case of constant eddy diffusivity. After some time, however, a weak thermocline is formed at a certain depth and gradually more pronounced with time until $n = 4$, while a relatively uniform buoyancy gradient is maintained within the upper mixed layer above the thermocline. Correspondingly, the maximum velocity shear appears near the thermocline and increases with time (Fig. 1b). The corresponding evolution of $E(z, t)$ shows that TKE (Fig. 1c) decreases rapidly with depth, reaching a minimum at the depth of the maximum buoyancy gradient, and the minimum level of TKE continues to decrease with time. Below the thermocline the initial turbulence still persists but dissipates slowly with time.

Transition in the development of the thermocline occurs at $n = 5$. At the thermocline the density gradient does not increase any more. Instead, its thickness grows

[1] The term "thermocline" in this paper always refers to a diurnal thermocline in the oceanic mixed layer.

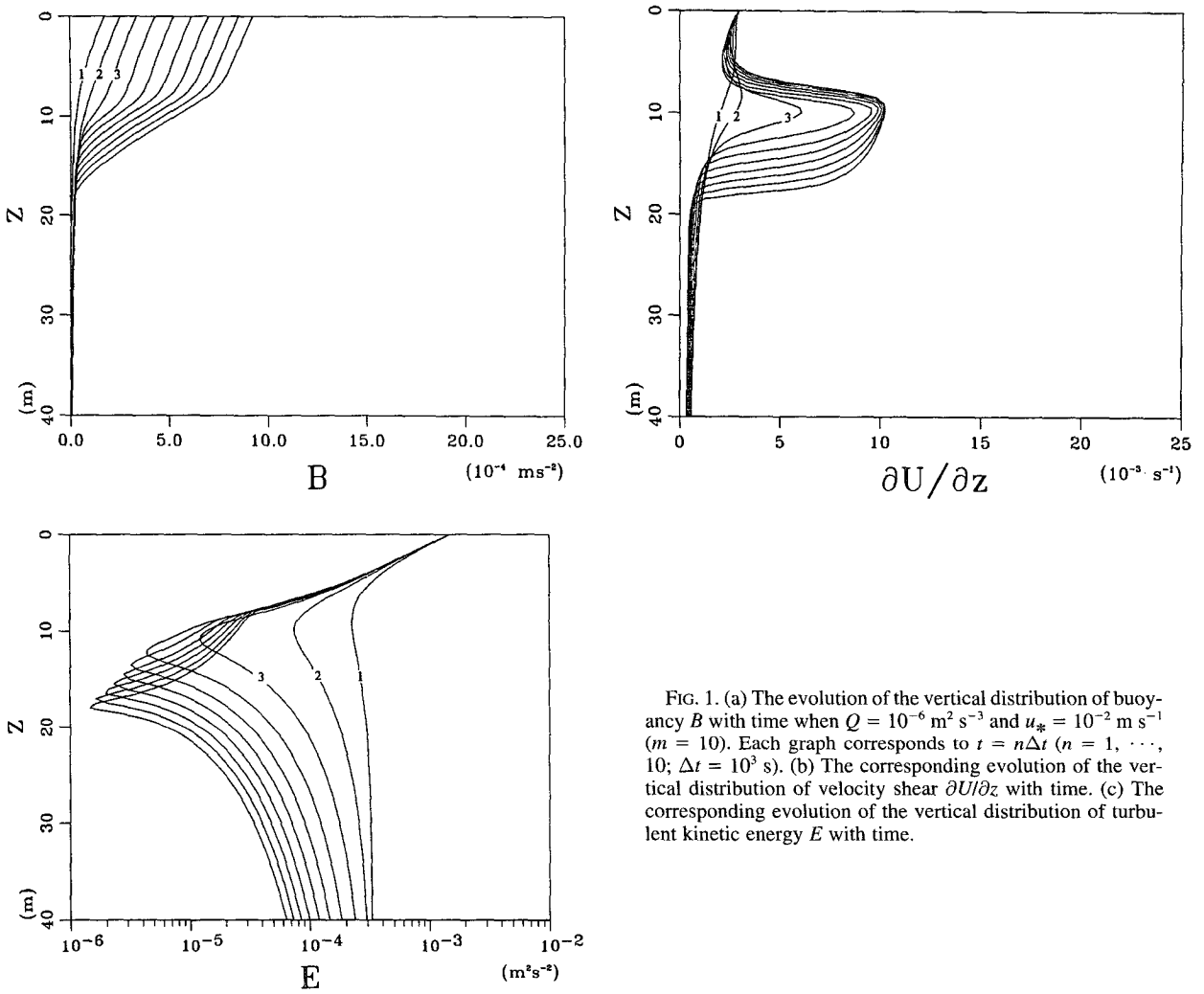

FIG. 1. (a) The evolution of the vertical distribution of buoyancy B with time when $Q = 10^{-6}$ m^2 s^{-3} and $u_* = 10^{-2}$ m s^{-1} ($m = 10$). Each graph corresponds to $t = n\Delta t$ ($n = 1, \cdots, 10$; $\Delta t = 10^3$ s). (b) The corresponding evolution of the vertical distribution of velocity shear $\partial U/\partial z$ with time. (c) The corresponding evolution of the vertical distribution of turbulent kinetic energy E with time.

with time. This result is contrary to the case of shear-free turbulence (Hopfinger and Linden 1982; Noh and Long 1990; Noh and Fernando 1991), where the thickness of a thermocline is invariant with time. Similar patterns occur for the evolution of the velocity shear profile. The minimum TKE keeps decreasing, but at increasing depths with time. Careful examination, however, reveals that TKE at a fixed depth below the thermocline increases with time approaching an equilibrium level, once the depth of the minimum TKE passes through.

The present result shows good agreement with observations by Brainerd and Gregg (1993a), who found that the diurnal thermocline grows in thickness with time, while maintaining the thickness of the upper mixed layer. The buoyancy gradients in the upper mixed layer ($N^2 \approx 2.2 \times 10^{-5}$ s^{-2}) and at the thermocline ($N^2 \approx 8.1 \times 10^{-5}$ s^{-2}) in the present simulation also have the same order of magnitude as those they measured in the ocean ($N^2 \approx 1.5 \times 10^{-5}$ s^{-2} and $N^2 \approx 5.4 \times 10^{-5}$ s^{-2}).

b. *Evolution of a thermocline without TKE flux ($m = 0$)*

When there is no TKE flux ($m = 0$), a thermocline having the maximum buoyancy and velocity gradients does not appear below the sea surface (Figs. 2a,b). Instead, the depth affected by the surface boundary condition ($\partial B/\partial z = \text{const}$) increases with time owing to turbulent diffusion (Fig. 2a). In Fig. 2c, E initially decreases due to P_b but tends to recover with time, approaching an equilibrium level for a given depth. Meanwhile, the velocity shear (Fig. 2b) near the sea surface increases sharply soon after the onset of buoyancy flux owing to the decreased eddy diffusivity by P_b, but decreases slowly afterward as momentum is transferred downward. The velocity shear below the

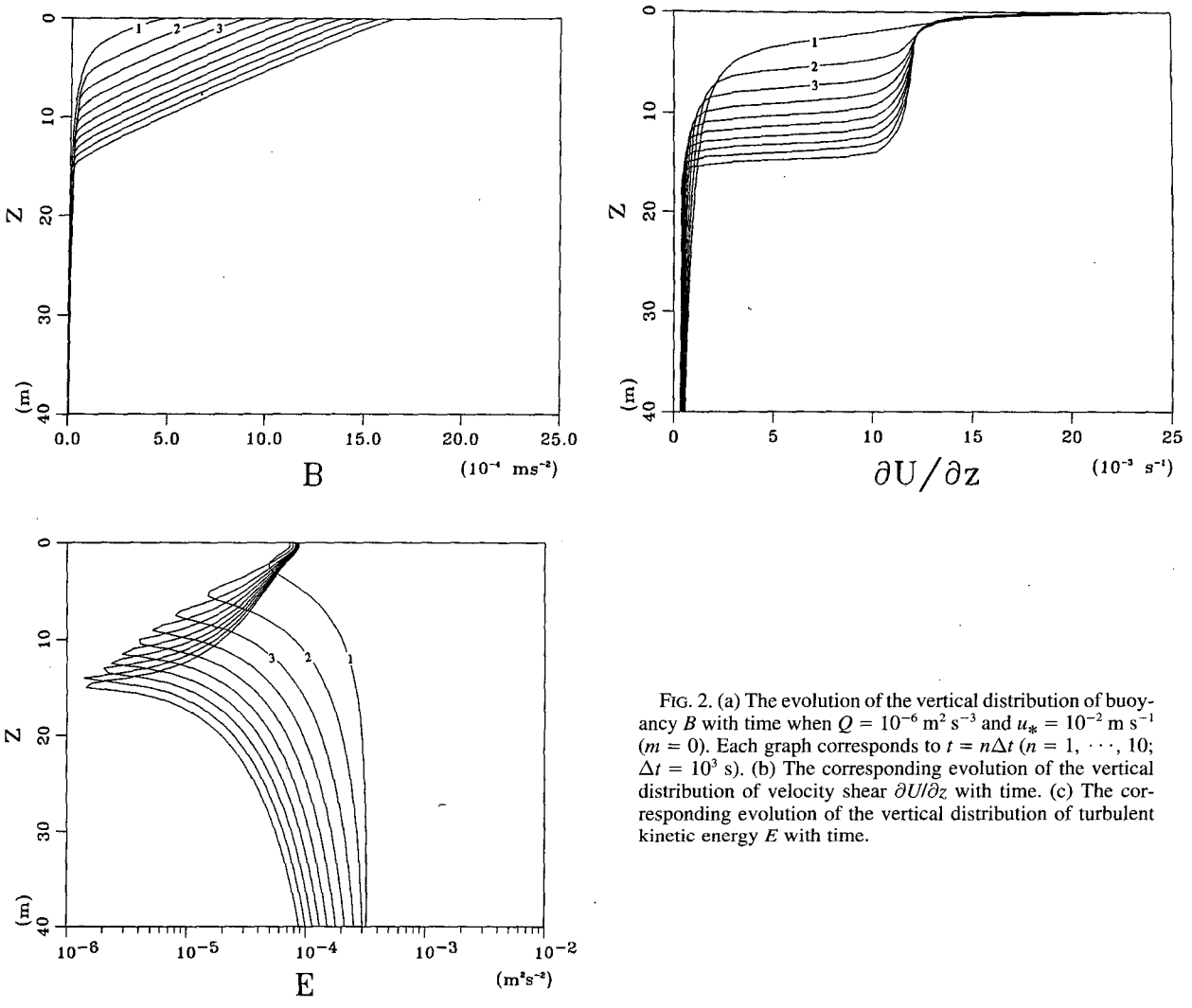

FIG. 2. (a) The evolution of the vertical distribution of buoyancy B with time when $Q = 10^{-6}$ m^2 s^{-3} and $u_* = 10^{-2}$ m s^{-1} ($m = 0$). Each graph corresponds to $t = n\Delta t$ ($n = 1, \cdots, 10$; $\Delta t = 10^3$ s). (b) The corresponding evolution of the vertical distribution of velocity shear $\partial U/\partial z$ with time. (c) The corresponding evolution of the vertical distribution of turbulent kinetic energy E with time.

surface increases due to momentum flux, approaching an equilibrium value, especially most rapidly at the depth of the minimum TKE and thus of the minimum eddy viscosity. Significantly, the time evolution of B, U, and E profiles has similar patterns to those observed below the thermocline at $n \geq 5$ in the case with TKE flux shown in Fig. 1.

c. *Mechanism for the formation of a thermocline*

The simulation results described above strongly suggest that the TKE flux plays a critical role that is indispensable for diurnal thermocline formation. To understand its role, it is necessary to consider the feedback mechanism between TKE flux (F) and buoyancy flux (P_b) and that between shear production (P_s) and buoyancy flux. These feedback mechanisms are shown schematically in Table 1.

If a stabilizing buoyancy is imposed on the surface, F is suppressed due to the stratification caused by P_b and TKE is reduced with depth accordingly. The local reduction of eddy diffusivity then induces even stronger stratification at a certain depth where F is suppressed further. This feedback mechanism leads to the formation of a thermocline across which both fluxes of TKE and buoyancy are prohibited. To illustrate this feedback mechanism, the time evolution of buoyancy and TKE profiles is calculated with TKE flux ($m = 10$) but with no velocity shear ($P_s = 0$) and is shown in Fig. 3. The TKE continues to decrease with time at the thermocline because the feedback mechanism between P_b and F continues to decrease the eddy diffusivity there. Below the thermocline the initial turbulence persists but dissipates slowly with time because the TKE flux across the thermocline is suppressed.

On the other hand, the stratification due to P_b increases the velocity shear by suppressing the momentum flux, and this increases P_s. Therefore, the TKE decreased by stratification and the TKE increased by

TABLE 1. Feedback mechanisms between P_b vs F and P_s.

P_b vs F:
buoyancy flux (P_b)
→ induce stratification ($|\partial B/\partial z|$ ⇑)
→ suppress TKE flux (F ⇓)
→ decrease eddy diffusivity (K ⇓)
→ increase stratification ($|\partial B/\partial z|$ ⇑)
•••
⇒ Positive feedback between $|\partial B/\partial z|$ and F leads to the formation of a thermocline.

P_b vs P_s:
buoyancy flux (P_b)
→ induce stratification ($|\partial B/\partial z|$ ⇑)
→ decrease eddy diffusivity (K ⇓)
→ increase velocity shear ($|\partial U/\partial z|$ ⇑)
→ increase eddy diffusivity (K ⇑)
•••
⇒ The local balance ($P_b + P_s - \epsilon = 0$) is approached without forming a thermocline

velocity shear lead to a local balance between P_s, P_b, and ϵ. This equilibrium maintains the eddy diffusivity at a certain level, which causes continuous penetration of heat and momentum fluxes instead of forming a thermocline.

The difference can be clearly understood by comparing Fig. 3b and Fig. 2c. In Fig. 3b, the feedback mechanism between F and P_b leads to a continuous decrease in E at the depth of thermocline formation. On the other hand, in Fig. 2c, the initial decrease in E due to P_b tends to recover with time, approaching an equilibrium level for a given depth, because it is followed by an increase in P_s.

To understand the case of section 3a where a thermocline is formed in the presence of both P_s and F, the budget of TKE is examined. Corresponding to the case of Fig. 1 at $n = 10$ (Fig. 4), F dominates over P_s as a turbulence source in the upper mixed layer. However, F vanishes at the thermocline depth, and P_s becomes the only source of turbulence below the thermocline. Measurements of the dissipation rate ϵ (Anis and Moum 1992; Osborn et al. 1992; Brainerd and Gregg 1993a) show that near the surface ϵ exceeds by up to ten times the value expected from shear production only, suggesting that turbulence production near the surface is dominated by TKE flux from the sea surface. In particular, in agreement with the present result, Brainerd and Gregg (1993a) found that the dissipation below the diurnal thermocline can be estimated by shear production only, whereas it is much larger in the upper mixed layer above the diurnal thermocline.

Based on this information it can be inferred that the feedback between F and P_b leads to the formation of a thermocline. In the presence of velocity shear, the increase of P_s at the thermocline maintains the eddy diffusivity at a certain level because of the balance between P_s, P_b, and ϵ (Fig. 3c), as in the case of no TKE flux (Fig. 2), although the TKE flux vanishes at the thermocline. The consequent finite eddy diffusivity facilitates growth of the thermocline thickness. A similar mechanism was suggested by Brainerd and Gregg (1993b), along with the penetration of solar radiation below the diurnal thermocline, to explain the growth of the thermocline thickness.

d. Comparison between the atmospheric boundary layer and the oceanic mixed layer under a stabilizing buoyancy flux

This remarkable contrast between the time evolution of buoyancy profiles with and without TKE flux (Fig.

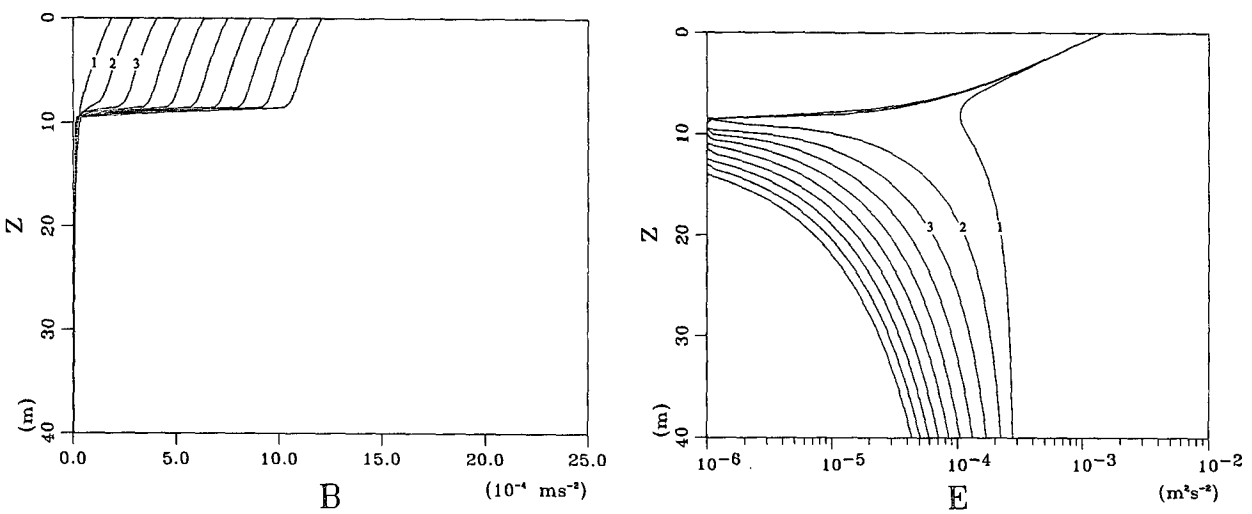

FIG. 3. (a) The evolution of the vertical distribution of buoyancy B with time when $Q = 10^{-6}$ m^2 s^{-3} and $u_* = 10^{-2}$ m s^{-1} ($m = 10$). The calculation was made without the velocity shear. Each graph corresponds to $t = n\Delta t$ ($n = 1, \cdots, 10$; $\Delta t = 10^3$ s). (b) The corresponding evolution of the vertical distribution of turbulent kinetic energy E with time.

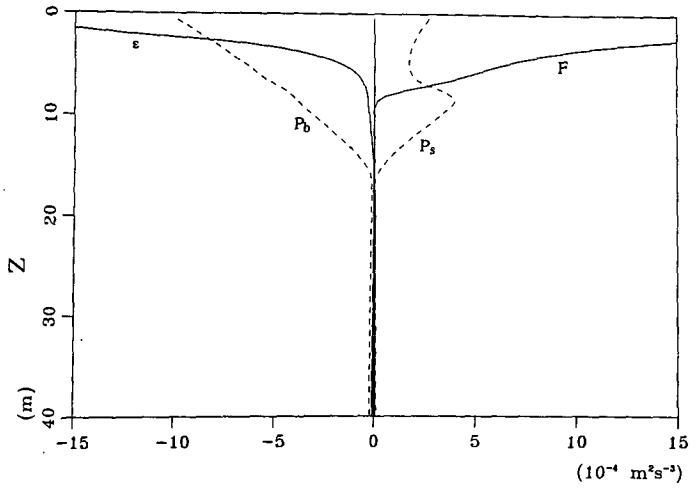

FIG. 4. The TKE budget when $u_* = 0.01$ m s^{-1} and $Q = 10^{-6}$ m^2 s^{-3} ($t = 10^4$ s); F is the TKE flux, P_s is the production of TKE by velocity shear, P_b is the decay of TKE by buoyancy flux, and ϵ is the dissipation. The storage term dE/dt is too small to appear at all depths compared to other terms.

1a and Fig. 2a) bears a striking resemblance to the response to a stabilizing buoyancy flux of the atmospheric and oceanic boundary layers (Fig. 5). It is well established that F is negligible compared to P_s near the surface in the atmospheric boundary layer (Wyngaard and Cote 1971; Stull 1988), whereas F is expected to be a dominant source of turbulence in the oceanic mixed layer as mentioned above. Thus, it can be inferred from this comparison that it may be the TKE flux that causes the lack of similarity between the oceanic mixed layer and the atmospheric boundary layer in their responses to a stabilizing buoyancy flux.

e. *The thermocline depth for the case m = 10*

The thermocline depth h is calculated by determining the equilibrium depths of the maximum buoyancy and velocity gradients, which in fact coincide, as shown in Figs. 1a and 1c. It also coincides with the depth where the TKE flux disappears, as shown in Fig. 4. Hence, h grows more slowly than predicted by the Monin–Obukhov length scale L ($=u_*^3/Q$); that is, the exponent α for the relation $h \sim L^\alpha$ is less than one (Fig. 6). The field data by Price et al. (1986), also shown in Fig. 6, shows good agreement with the numerical results. The calculations of the shear-free case ($P_s = 0$) suggest that the presence of velocity shear does not have a significant effect on the thermocline depth, as can be seen from the comparison of Fig. 1 and Fig. 3. The presence of P_s increases h by less than 10%, but its effect becomes slightly larger at larger L.

The prediction of the depth of a diurnal thermocline was attempted from the bulk model by Niiler and Kraus (1977). The integration of (2.3) over the mixed layer of thickness h gives

$$\int_0^h \frac{\partial E}{\partial t}\,dz = mu_*^3 + \frac{1}{2}U^2\frac{\partial h}{\partial t} - \frac{1}{2}hQ - \frac{1}{2}hB\frac{\partial h}{\partial t} - D, \quad (3.1)$$

where $B = U = 0$ are assumed below the thermocline and D is the total dissipation within the mixed layer such that

$$D = \int_0^h \epsilon dz. \quad (3.2)$$

To derive (3.1) the velocity and buoyancy are assumed to be uniform within the mixed layer, as is always the case in bulk models. To close (3.1) Niiler and Kraus (1977) assumed that a fraction of each turbulence production term contributes to the total dissipation; that is,

$$D = m_* u_*^3 + \frac{m_s}{2}U^2\frac{\partial h}{\partial t} - \frac{m_e}{4}h(|Q| - Q), \quad (3.3)$$

where m_*, m_s, and m_e are constants representing the fraction of each turbulence production term. If the conditions $\partial h/\partial t = 0$ and $\partial E/\partial t = 0$ are applied to the case of diurnal thermocline formation ($Q > 0$), substitution of (3.3) for D in (3.1) gives

$$m_1 u_*^3 - (h/2)Q = 0, \quad (3.4)$$

with $m_1 = m - m_*$. This yields the depth of a diurnal thermocline as

$$h = 2m_1 L. \quad (3.5)$$

One dubious consequence implied by the hypothesis (3.3) is that D is independent of h in this situation, which is contrary to our intuition. The calculation ac-

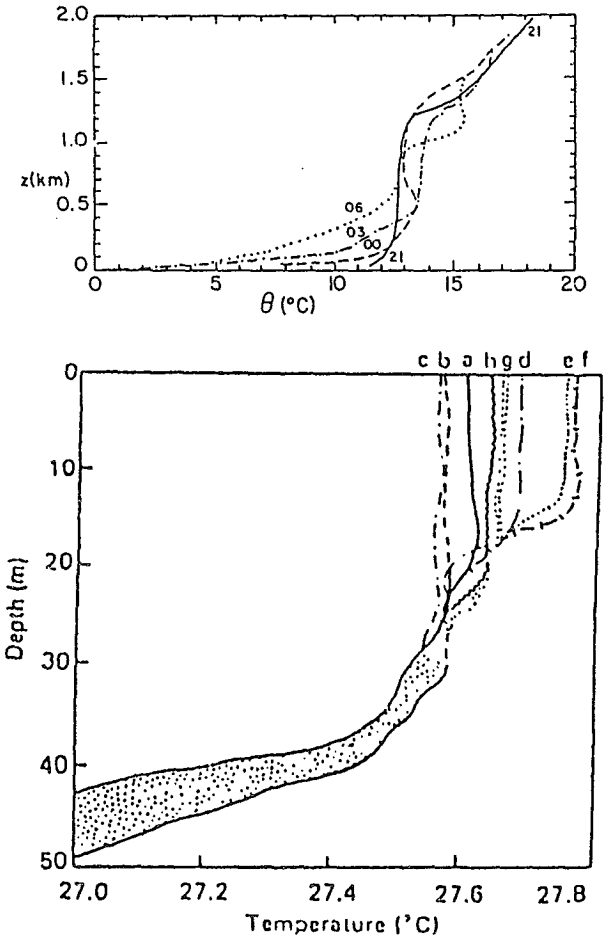

FIG. 5. (a) The diurnal variation of a potential temperature profile in the atmospheric boundary layer during Wangara Experiment (Arya 1988). (b) The diurnal variation of a temperature profile in the oceanic mixed layer during BOMEX (Delnore 1972); a-02, b-05, c-08, d-11, e-14, f-17, g-21, h-23.

tually reveals that D increases weakly with L (Fig. 7) and thus with h (see Fig. 6). This relationship tends to hinder the linear increase of h with L.

f. The flux Richardson number at the thermocline

One remarkable property of the model results is that Rf remains constant at the thermocline once it is formed, and this critical Rf number, Rf_c, nearly equals unity, independent of Q and u_* (Fig. 8).

As the TKE flux disappears at the thermocline (see Fig. 4), the TKE budget is balanced among P_s, P_b, and ϵ. That is,

$$P_s - P_b - \epsilon = 0 \tag{3.6}$$

or

$$\mathrm{Rf} = 1 - \epsilon/P_s \tag{3.7}$$

$$= 1 - \frac{C}{S}\left[\frac{q^2 l^{-2}}{(\partial U/\partial z)^2}\right]. \tag{3.8}$$

Using (2.12) and (2.13), (3.8) can be rewritten as

$$\mathrm{Rf} = 1 - \frac{C_0}{S_0}(1 + c_1\,\mathrm{Rt})\left[\frac{q^2 l^{-2}}{(\partial U/\partial z)^2}\right]. \tag{3.9}$$

When Rt becomes large at the thermocline due to the decrease of TKE and the increase of stratification (see Figs. 1a and 1c), (3.9) reduces to

$$\mathrm{Rf} = 1 - \frac{C_0}{S_0} c_1\left[\frac{N^2}{(\partial U/\partial z)^2}\right] \tag{3.10}$$

$$= 1 - (C_0/S_0)c_1\,\mathrm{Pr}\,\mathrm{Rf}. \tag{3.11}$$

That is,

$$\mathrm{Rf} = [1 + (C_0/S_0)c_1\,\mathrm{Pr}]^{-1}. \tag{3.12}$$

This gives a constant value of the critical flux Richardson number, $\mathrm{Rf}_c = 0.96$.

The flux Richardson number at the thermocline maintains a constant value of nearly unity in the field data (Halpern 1974; Padman and Jones 1985), and it has been often used as a basic assumption in many bulk models (Pollard et al. 1973; Garwood 1977). It is reassuring to find from the present numerical simulation that the constant flux Richardson number of nearly unity is actually maintained at the thermocline during its formation. It is also observed that Rf ($=P_b/P_s$) is usually larger than unity within the mixed layer. The production of TKE by both F and P_s balances its decay by P_b and ϵ; that is,

$$F + P_s = P_b + \epsilon, \tag{3.13}$$

and it is usually F that dominates the production within the mixed layer so that P_s becomes smaller than P_b.

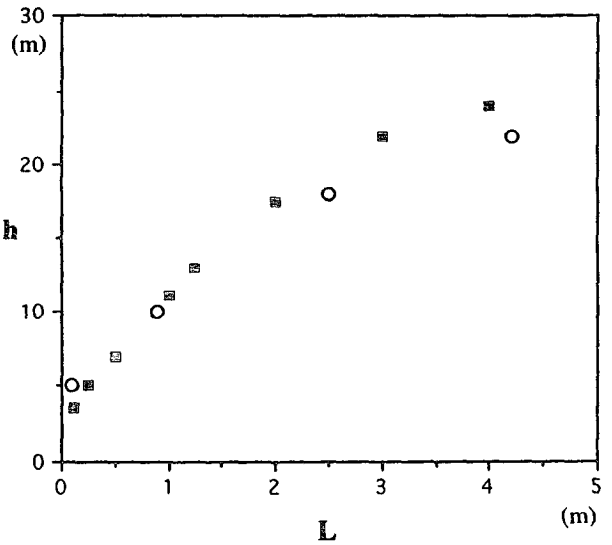

FIG. 6. The variation of the depth of a thermocline h with the Monin–Obukhov length scale L: ■, the model results; ○, the observation data by Price et al. (1986) (Fig. 6 in their paper).

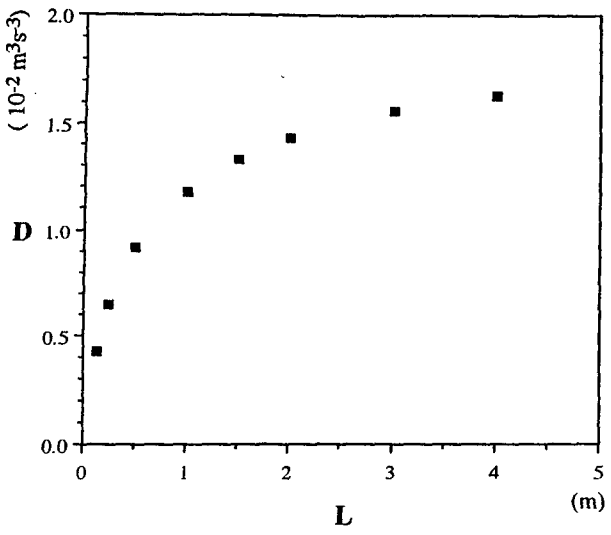

FIG. 7. The variation of the total dissipation within the mixed layer D with L.

4. The effects of Coriolis force and the penetration of solar radiation

The effects of Coriolis force and the penetration of solar radiation into the deeper region have been excluded to clarify the fluid dynamical process leading to the formation of a diurnal thermocline from the interaction between the TKE flux and density stratification. The penetration of solar radiation, which is independent of fluid dynamical process such as turbulence and stratification, affects temperature profiles unilaterally, so it cannot trigger the feedback mechanism described in section 3c. The only contribution of Coriolis force to the formation of a diurnal thermocline is the minor modification of P_s in the TKE equation (2.6) at a depth greater than the Ekman length scale since it makes no direct contribution to TKE (Phillips 1977). Therefore, these factors do not affect whether a diurnal thermocline is formed or not, although they may affect the thickness and depth of a diurnal thermocline. Moreover, the typical Ekman length scale L_E in this case is estimated as $L_E \sim u_*/f \sim 10^2$ m, since $u_* \sim 10^{-2}$ m s^{-1} and $f \sim 10^{-4}$ s^{-1}, and it is significantly larger than the typical values of h, which renders the Coriolis force even less important.

The equations for U and B (2.4) and (2.5) can be extended to include the effects of Coriolis force and the penetration of solar radiation:

$$\frac{\partial U}{\partial t} = \frac{\partial}{\partial z}\left(K\frac{\partial U}{\partial z}\right) + fV \tag{4.1}$$

$$\frac{\partial V}{\partial t} = \frac{\partial}{\partial z}\left(K\frac{\partial V}{\partial z}\right) - fU \tag{4.2}$$

$$\frac{\partial B}{\partial t} = \frac{\partial}{\partial z}\left(K_B\frac{\partial B}{\partial z}\right) - \frac{\partial R}{\partial z}, \tag{4.3}$$

where V is the mean velocity in the y direction, f is the Coriolis parameter, and R is the buoyancy flux due to the radiative flux penetrating to depth z. The boundary conditions are

$$K\frac{\partial U}{\partial z} = u_*^2 \tag{4.4}$$

$$K\frac{\partial V}{\partial z} = 0 \tag{4.5}$$

$$K_B\frac{\partial B}{\partial z} + R = Q. \tag{4.6}$$

Radiative flux is parameterized following Paulson and Simpson (1977). The equation and boundary condition for TKE as well as the turbulence parameterizations remain the same as in section 2.

As is expected, no significant differences are observed in the results, Fig. 9 compared to Fig. 1, except for the slightly deeper penetration of buoyancy owing to the radiative flux and the mean horizontal velocity fields affected by the Coriolis force.

5. Conclusions and discussion

The dynamical process of the formation of a diurnal thermocline in the oceanic mixed layer has been elu-

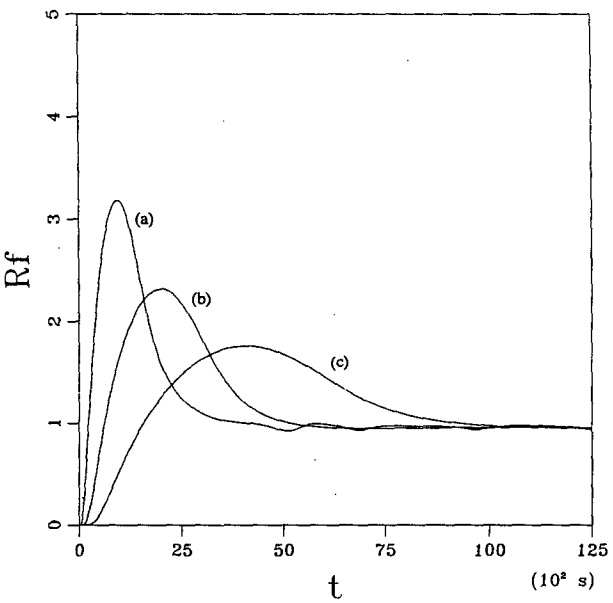

FIG. 8. The variation of the flux Richardson number at the thermocline with time: $u_* = 10^{-2}$ m s^{-1}; (a) $Q = 10^{-6}$ m^2 s^{-3}, (b) $Q = 5 \times 10^{-7}$ m^2 s^{-3}, (c) $Q = 2.5 \times 10^{-7}$ m^2 s^{-3}. Similar graphs are obtained with the variation of u_* for a given Q.

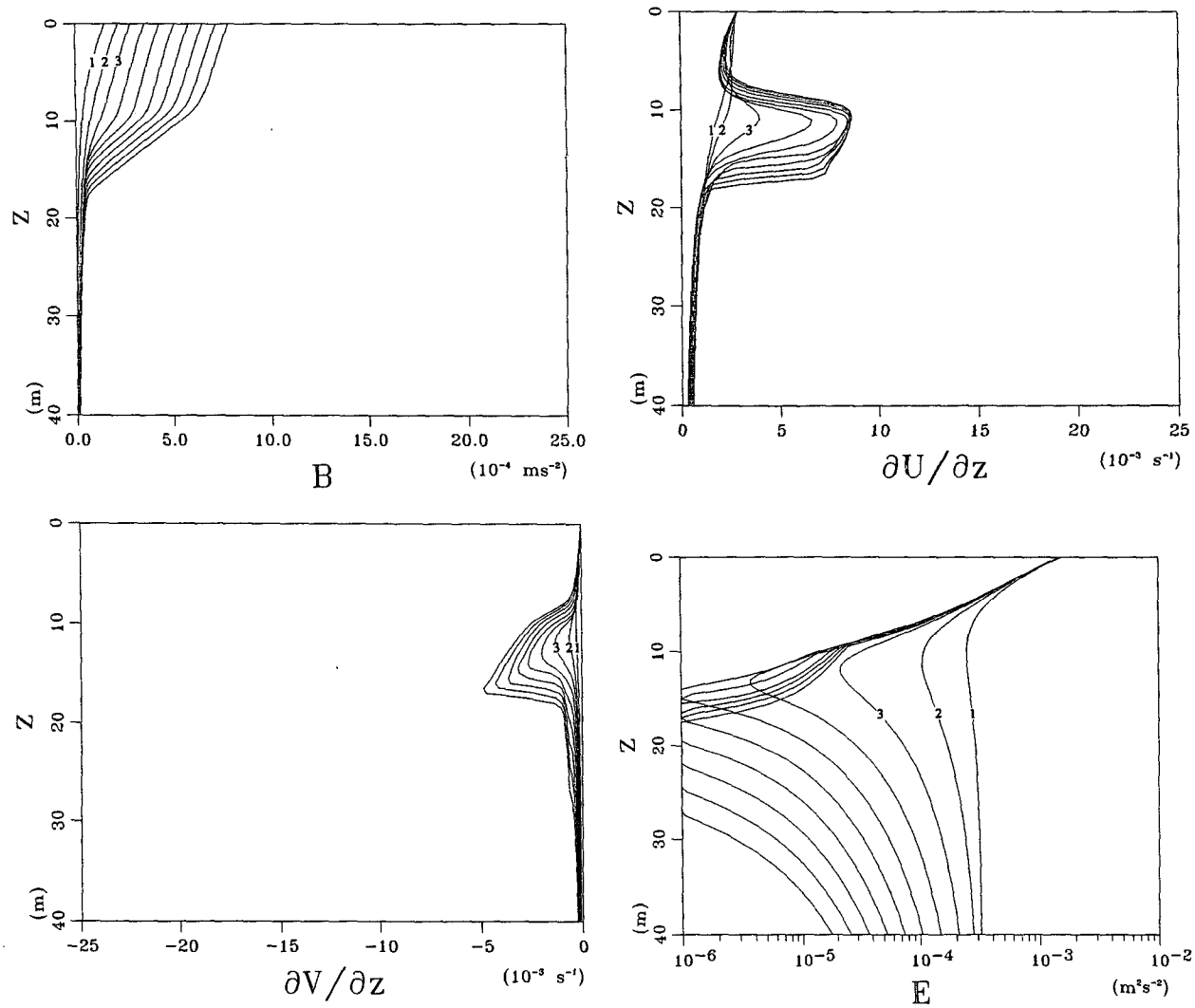

FIG. 9. (a) The evolution of the vertical distribution of buoyancy B with time when $Q = 10^{-6}$ m^2 s^{-3} and $u_* = 10^{-2}$ m s^{-1} ($m = 10$). The calculation included the effects of Coriolis force and the penetration of solar radiation. Each graph corresponds to $t = n\Delta t$ ($n = 1 \cdots 10$, $\Delta t = 10^3$ s). (b) The corresponding evolution of the vertical distribution of velocity shear $\partial U/\partial z$ with time. (c) The corresponding evolution of the vertical distribution of velocity shear $\partial V/\partial z$ with time. (d) The corresponding evolution of the vertical distribution of turbulent kinetic energy E with time.

cidated from a simple turbulence model. The important results are as follows:

(i) The flux of TKE plays a critical role without which the formation of a thermocline is not possible.

(ii) The divergence of TKE flux is a dominant source of turbulence in the upper mixed layer above the diurnal thermocline, but it vanishes at the diurnal thermocline.

(iii) Below the diurnal thermocline turbulence is maintained by the balance between shear production, buoyancy flux, and dissipation; this causes the growth of the diurnal thermocline thickness.

(iv) It is the importance of TKE flux that causes the lack of similarity between the oceanic mixed layer and the atmospheric boundary layer in their responses to a diurnal stabilizing buoyancy flux.

(v) The depth of the diurnal thermocline is observed to increase more slowly than predicted by the Monin–Obukhov length scale L.

(vi) The flux Richardson number Rf at the diurnal thermocline maintains a constant value of nearly unity ($\mathrm{Rf}_c = 0.96$), regardless of the conditions of Q and u_* at the sea surface.

The overall results are in good agreement with the observations by Brainerd and Gregg (1993a).

The assumption of the local balance, $P_s - P_b - \epsilon = 0$, is widely used in the ocean, for example, in the level-2 model of Mellor and Yamada (1982) or for the

estimation of eddy diffusivity from this relation (Osborn 1980). However, according to the present results it may not be justified in the upper ocean above the diurnal thermocline, and thus this assumption needs to be justified carefully before application.

In the present model, the effect of stratification on the eddy viscosity K was parameterized by the Richardson number for turbulent eddies Rt $[= -(\partial B/\partial z)l^2/q^2]$, and it decreases to zero continuously with increasing stratification. This is different from the Mellor and Yamada model (1982), in which K becomes zero abruptly at Rf = 0.19. The latter could not be used in the present model since Rf is usually greater than unity within the mixed layer, as mentioned in section 3e.

The total dissipation over the mixed layer increases with increasing depth of the mixed layer, which contradicts the hypothesis used in the bulk models such as Niiler and Kraus (1977) and Garwood (1977). Consequently, the strict proportionality of the depth of a diurnal thermocline to the Monin–Obukhov length scale, $h \propto L$, based on this hypothesis was not observed.

It was also noted that the buoyancy flux still exists, even if the depth of a thermocline remains stationary, as evident from Fig. 1 and Fig. 4, and the buoyancy flux increases the buoyancy below the thermocline slowly with time. The buoyancy flux at the base of the mixed layer is due to both entrainment and turbulent diffusion, although the latter is usually negligible during the deepening of the mixed layer. Therefore, the conventional parameterization in bulk models for the buoyancy flux at the bottom of the mixed layer

$$-\overline{bw}(z = h) = B\partial h/\partial t \qquad (5.1)$$

and similarly that for the momentum flux

$$-\overline{uw}(z = h) = U\partial h/\partial t, \qquad (5.2)$$

which were also used to derive (3.1), are not always justified.

The present model is somewhat similar to the bulk models rather than most other turbulence models, in that the TKE flux plays a dominant role in the dynamics of the mixed layer. The dominance of the production of TKE by velocity shear P_s is related to the choice of length scale of turbulence as $l \sim \kappa z$ (with negligible z_0) in most turbulence models. The length scale causes unrealistically large buoyancy and velocity gradients within the mixed layer in turbulence models, and therefore large P_s, contrary to the bulk models, which have uniform buoyancy and velocity distributions within a mixed layer. Good agreement between the numerical results and field measurements in the buoyancy gradients within the upper mixed layer and at the diurnal thermocline (see section 3a), and in the depth of a diurnal thermocline (see section 3e) demonstrate that the length scale used in the model presented is within a reasonable range. Interestingly, Cane (1993) suggested that the discrepancy between turbulence models and bulk models can be reduced by increasing the length scale of turbulence in the turbulence model. The presence of convection in a thin surface layer under the influence of stabilizing buoyancy flux (Woods and Barkmann 1986) and Langmuir circulation (Leibovich 1983) also suggest large-scale mixing near the sea surface. Further study may be required, however, to clarify the discrepancies that remain between these two different approaches to modeling of the oceanic mixed layer.

Acknowledgments. The author wishes to thank Prof. O. M. Phillips of The Johns Hopkins University for his careful comments and helpful suggestions. I have also benefited from various support provided by Prof. J. W. Kim and help in preparing the manuscript provided by Ms. W. S. Lee. This research was supported by Korea Science and Engineering Foundation and by the Ministry of Education of Korea.

REFERENCES

Andre, J. C., and P. Lacarrere, 1985: Mean and turbulent structure of the oceanic surface layer as determined from one-dimensional third-order simulations. *J. Phys. Oceanogr.*, **15**, 121–132.

——, G. De Moor, P. Lacarrere, G. Therry, and R. du Vachat, 1978: Modeling the 24-hour evolution of the mean and turbulent structures of the planetary boundary layer. *J. Atmos. Sci.*, **35**, 1861–1883.

Anis, A., and J. N. Moum, 1992: The superadiabatic surface layer of the ocean during convection. *J. Phys. Oceanogr.*, **22**, 1221–1227.

Arya, S. P., 1988: *Introduction to Micrometeorology.* Academic Press, 59 pp.

Blackadar, A. K., 1962: The vertical distribution of wind and turbulent exchange in neutral atmosphere. *J. Geophys. Res.*, **67**, 3095–3102.

Brainerd, K. E., and M. C. Gregg, 1993a: Diurnal restratification and turbulence in the oceanic surface mixed layer: 1. Observation. *J. Geophys. Res.*, **98**, 22 645–22 656.

——, and ——, 1993b: Diurnal restratification and turbulence in the oceanic surface mixed layer: 2. Modeling. *J. Geophys. Res.*, **98**, 22 657–22 664.

Britter, R. E., J. C. R. Hunt, G. L. Marsh, and W. H. Snyder, 1983: The effects of stable stratification on turbulent diffusion and the decay of grid turbulence. *J. Fluid Mech.*, **127**, 27–44.

Cane, M. A., 1993: Near-surface mixing and the ocean's role in climate. *Large Eddy Simulation of Complex Engineering and Geophysical Flows,* B. Galperin and S. Orszag, Eds., Cambridge Press, 489–509.

Csanady, G. T., 1964: Turbulent diffusion in a stratified fluid. *J. Atmos. Sci.*, **21**, 439–447.

Davies, A. M., and J. E. Jones, 1988: Modelling turbulence in shallow sea regions. *Small-Scale Turbulence and Mixing in the Ocean,* J. C. J. Nihoul and B. M. Jamart, Eds., Elsevier, 63–76.

Delnore, V. E., 1972: Diurnal variations of temperature and energy budget for the oceanic mixed layer. *J. Phys. Oceanogr.*, **2**, 239–247.

Denman, K. L., and M. Miyake, 1973: Upper layer modification at ocean station Papa: Observations and simulation. *J. Phys. Oceanogr.*, **3**, 185–196.

Galperin, B., L. H. Kantha, S. Hassid, and A. Rosati, 1988: A quasi-equilibrium turbulent kinetic energy model for geophysical flows. *J. Atmos. Sci.*, **45**, 55–62.

Garwood, R. W., 1977: An oceanic mixed layer model capable of simulating cyclic states. *J. Phys. Oceanogr.*, **7**, 455–468.

——, 1979: Air–sea interaction and dynamics of the surface mixed layer. *Rev. Geophys. Space Phys.*, **17,** 1507–1521.

——, 1987: Unsteady shallowing mixed layer. *Dynamics of the Oceanic Surface Mixed Layer,* P. Müller and D. Henderson, Eds., University of Hawaii at Manoa, 119–130.

Gaspar, P., 1988: Modeling the seasonal cycle of the ocean. *J. Phys. Oceanogr.*, **18,** 161–180.

Halpern, D., 1974: Observations of the deepening of the wind-mixed layer in the northeast Pacific Ocean. *J. Phys. Oceanogr.*, **4,** 454–466.

Hopfinger, E. J., 1987: Turbulence in stratified fluids: A review. *J. Geophys. Res.*, **92,** 5287–5303.

——, and P. F. Linden, 1982: Formation of thermoclines in zero mean-shear turbulence subjected to a stabilizing buoyancy flux. *J. Fluid Mech.*, **78,** 155–175.

Imberger, J., 1985: The diurnal mixed layer. *Limnol. Oceanogr.*, **30,** 737–770.

Kim, J. W., 1976: A generalized bulk model of the oceanic mixed layer. *J. Phys. Oceanogr.*, **6,** 686–695.

Kitaigorodskii, S. A., 1970: *The Physics of Air–Sea Interaction.* Israel Program for Scientific Translation, 237 pp.

Klein, P., and M. Coantic, 1981: A numerical study of turbulent process in the marine upper layers. *J. Phys. Oceanogr.*, **11,** 849–863.

Kraus, E. B., 1988: Merits and defects of different approaches to mixed layer modelling. *Small-Scale Turbulence and Mixing in the Ocean,* J. C. J. Nihoul and B. M. Jamart, Eds., Elsevier, 37–50.

——, and J. S. Turner, 1967: A one-dimensional model of the seasonal thermocline. *Tellus,* **19,** 98–106.

——, R. Bleck, and H. P. Hanson, 1988: The inclusion of a surface mixed layer in a large-scale circulation model. *Small-Scale Turbulence and Mixing in the Ocean,* J. C. J. Nihoul and B. M. Jamart, Eds., Elsevier, 51–62.

Kundu, P. J., 1980: A numerical investigation of mixed-layer dynamics. *J. Phys. Oceanogr.*, **10,** 220–236.

Leibovich, S., 1983: The form and dynamics of Langmuir circulation. *Ann. Rev. Fluid Mech.*, **15,** 391–427.

Mellor, G. L., and P. A. Durbin, 1975: The structure and dynamics of the ocean surface mixed layer. *J. Phys. Oceanogr.*, **5,** 718–728.

——, and T. Yamada, 1982: Development of a turbulent closure model for geophysical fluid problems. *Rev. Geophys. Space Phys.*, **20,** 851–875.

Niiler, P. P., and E. B. Kraus, 1977: One-dimensional models of the upper ocean. *Modelling and Prediction of the Upper Layers of the Ocean,* E. B. Kraus, Ed., Pergamon Press, 143–172.

Noh, Y., 1993: A numerical model for the onset of stratification in shear-free turbulence. *Geophys. Astrophys. Fluid Dyn.*, **72,** 35–56.

——, and R. R. Long, 1990: Turbulent mixing in a rotating, stratified fluid. *Geophys. Astrophys. Fluid Dyn.*, **53,** 125–143.

——, and H. J. S. Fernando, 1991: A numerical study on the formation of a thermocline in shear-free turbulence. *Phys. Fluids A,* **3,** 422–426.

Osborn, T. R., 1980: Estimates of the local rate of vertical diffusion from dissipation measurements. *J. Phys. Oceanogr.*, **10,** 83–89.

Osborn, T., D. M. Farmer, S. Vagle, S. A. Thorpe, and M. Cure, 1992: Measurements of bubble plumes and turbulence from a submarine. *Atmos.–Ocean,* **30,** 419–440.

Padman, L., and I. S. F. Jones, 1985: Richardson number statistics in the seasonal thermocline. *J. Phys. Oceanogr.*, **15,** 844–854.

Paulson, C. A., and J. J. Simpson, 1977: Irradiance measurements in the upper ocean. *J. Phys. Oceanogr.*, **7,** 952–956.

Phillips, O. M., 1977: *The Dynamics of the Upper Ocean.* Cambridge University Press, 256–295.

Pollard, R. T., P. B. Rhines, and R. O. R. Y. Thompson, 1973: The deepening of the wind mixed layer. *Geophys. Fluid Dyn.*, **7,** 298–300.

Price, J. F., R. A. Weller, and R. Pinkel, 1986: Diurnal cycling: Observations and models of the upper ocean response to diurnal heating, cooling and wind mixing. *J. Geophys. Res.*, **91,** 8411–8427.

Schudlich, R. R., and J. F. Price, 1992: Diurnal cycles of current, temperature and turbulent diffusion in a model of the equatorial upper ocean. *J. Geophys. Res.*, **97,** 5409–5422.

Stillinger, D. C., K. N. Helland, and C. W. van Atta, 1983: Experiments on the stratification of homogeneous turbulence to internal waves in a stratified fluid. *J. Fluid Mech.*, **131,** 91–122.

Stommel, H., K. Saunders, W. Simmons, and J. Cooper, 1969: Observation of the diurnal thermocline. *Deep-Sea Res.*, **16,** 269–284.

Stull, R. B., 1988: *An Introduction to Boundary Layer Meteorology.* Kluwer Academic, 499–543.

Turner, J. S., 1981: Small-scale mixing processes. *Evolution of Physical Oceanography,* B. A. Warren and C. Wunsch, Eds., 236–263.

Woods, J. D., and W. Barkmann, 1986: The response of the upper ocean to solar heating: I. The mixed layer. *Quart. J. Roy. Meteor. Soc.*, **112,** 1–27.

Wyngaard, J. C., and O. R. Cote, 1971: The budget of turbulent kinetic energy and temperature variance in the atmospheric boundary layer. *J. Atmos. Sci.*, **28,** 190–201.

Yamada, T., and G. Mellor, 1975: A simulation of the Wangara atmospheric boundary layer data. *J. Atmos. Sci.*, **32,** 2309–2329.

Yu, L., and J. J. O'Brien, 1991: Variational estimation of the wind stress drag coefficient and the oceanic eddy viscosity profile. *J. Phys. Oceanogr.*, **21,** 709–718.